

# Circular Patch Microstrip Array Antenna for KU-band

T.F.Lai, Wan Nor Liza Mahadi, Norhayati Soin

**Abstract**—This paper present a circular patch microstrip array antenna operate in KU-band (10.9GHz – 17.25GHz). The proposed circular patch array antenna will be in light weight, flexible, slim and compact unit compare with current antenna used in KU-band.

The paper also presents the detail steps of designing the circular patch microstrip array antenna. An Advance Design System (ADS) software is used to compute the gain, power, radiation pattern, and  $S_{11}$  of the antenna. The proposed Circular patch microstrip array antenna basically is a phased array consisting of 'n' elements (circular patch antennas) arranged in a rectangular grid. The size of each element is determined by the operating frequency. The incident wave from satellite arrives at the plane of the antenna with equal phase across the surface of the array. Each 'n' element receives a small amount of power in phase with the others. There are feed network connects each element to the microstrip lines with an equal length, thus the signals reaching the circular patches are all combined in phase and the voltages add up.

The significant difference of the circular patch array antenna is not come in the phase across the surface but in the magnitude distribution.

**Keywords**—Circular patch microstrip array antenna, gain, radiation pattern, S-Parameter.

## I. INTRODUCTION

CURRENTLY, parabolic dish antenna is at its own pace to receive the KU-band signals. The dish provides the best compromise of high gain, which is about 37dB at 12.5GHZ for 0.6m diameter, 38.5 dB for 0.75m and 40.3 dB for 0.9m [1]. A paraboloid can be considered as a three dimensional profile produced by rotating the parabola about its central axis. In receiving mode, the parabolic shape reflects signals, impinges on its surface to the focal point. In general, the working principle of a parabolic reflector is that a plane wavefront transmitted from satellite would be reflected from the dish surface and converted to a spherical wavefront. A waveguide positioned at the focal point collects the signals [2].

However, it is not necessary that only parabolic dish can be used to receive the KU-band signals, the circular patch microstrip array antenna also can be used to receive the KU-band signals [3]. The proposed antenna has 36 elements arranged in a rectangular grid form and operated in  $TM_{11}$  mode [4]. Each element has an equal radius and a separation distance from their neighbours. The working principle of this antenna is that the conduction surface is face directly to the

incoming signals. The voltage will be equally distributed among all the elements. The voltage may superimpose and cancel each other due to the phase different. Hence the resultant voltage appears at the feed point. The microstrip feed networks are designed to do the task of collecting all the induced voltages fed into one point [5].

Comparing the circular patch microstrip array antenna with parabolic dish, it has some advantages such as small dimensions, light weight, slim size and easy manufacturing [6].

## II. THE DESIGN ISSUE OF CIRCULAR PATCH MICROSTRIP ARRAY ANTENNA

The design of circular patch microstrip array antenna will begin from single element. It then developed into 36 elements and finally the total radiation pattern, gain and S-parameter is computed through ADS.

### A. Circular patch antenna analysis

From the literature review, the effective radius of circular patch is found by [7]:

$$r_{eff} = r \sqrt{1 + \frac{2h}{\pi r \epsilon_r} \left[ \ln \left( \frac{\pi r}{2h} \right) + 1.7726 \right]} \quad (1)$$

Where  $r$  = physical radius of circular patch  
 $h$  = height or thickness of the substrate  
 $\epsilon_r$  = dielectric constant

The effective area of the patch is then given by [8]:

$$A_{eff} = \pi r_{eff}^2 \quad (2)$$

### B. Resonant frequency of the circular patch

The resonant frequencies of the circular patch can be analysed conveniently using the cavity model [9], [10], [11]. The cavity is composed of two perfect electric conductors at the top and bottom to represent the patch and the ground plane, and a cylindrical perfect magnetic conductor around the circular periphery of the cavity.

Using the synthesis procedure as mentioned in [12], the resonant frequency of a circular patch can be computed as:

$$f_0 = \frac{cJ_{mn}}{2\pi r_{eff} \sqrt{\epsilon_r}} \quad (3)$$

Where  $f_0$  = resonant frequency

$J_{mn}$  =  $m$ th zero of the derivative of the Bessel function or order  $n$

For dominant mode  $TM_{11}$ ,  $J_{mn} = 1.84118$  [13] which is extensively used in all kind of microstrip antennas.

C. Quality factor, Bandwidth, directivity and efficiency of the circular patch

The quality factor, bandwidth and efficiency are antenna figures of merit, which are interrelated, and there is no complete freedom to independently optimize each one. Therefore there is always a trade off between them in arriving at an optimum antenna performance. Often, however, there is a desire to optimize one of them while reducing the performance of the other.

The quality factor is a figure-of-merit that is representative of the antenna losses. For circular patch antenna, the total quality factor  $Q_t$  in general can be written as [14]:

$$\frac{1}{Q_t} = \frac{1}{Q_{rad}} + \frac{1}{Q_C} + \frac{1}{Q_d} \quad (4)$$

Where  $Q_{rad}$  = quality factor due to space wave losses

$Q_d$  = quality factor due to dielectric losses

$Q_C$  = quality factor due to ohmic losses

The fractional bandwidth of the circular patch is inversely proportional to the  $Q_t$  [15]. Another more meaningful definition of the fractional bandwidth is over a band of frequencies where the VSWR at the input terminals is equal to or less than a desired maximum value, assuming that the VSWR is unity at the design frequency. Then taking into account of the impedance matching, we have [16]

$$Bandwidth = \frac{VSWR - 1}{Q_t \sqrt{VSWR}} \quad (5)$$

Note that expression 5 can be applied for rectangular patch antenna as well. The dielectric loss due to quality factor in the circular patch for two commonly used materials can be obtained from table 1 [17].

The directivity of the circular is a measurement of the directional properties compared with those isotropic antennas. The tedium of numerical effort required to calculate the directivity of microstrip antenna has been addressed. The directivity of a circular microstrip antenna was computed by Derneryd [18]. The computation of directivity is complicated as the expression involving integral contains the Bessel functions.

TABLE I  
DIELECTRIC LOSS FOR RT-DUROID & ALUMINA

	RT-Duroid	Alumina
$\tan \delta$	$1 \times 10^{-3}$	$1.5 \times 10^{-4}$
$f$	$\text{dB/m} \times 10^{-3}$	$\text{dB/m} \times 10^{-4}$
1GHz	3.95	8.24
10GHz	39.5	82.4
20GHz	79	165

Recently Mahony [19] has simplified the computation by using the integral containing the Struve function. However it requires tabulated data of Struve function and therefore, the expression is not convenient for the fast calculation.

D. An array of circular patches

36 of circular patch antennas can be arranged into an array at which each row and column of array consisting of 6 elements. Fig. 1 shows a  $m \times n$  array and consider the antenna face to  $z$ -plane:

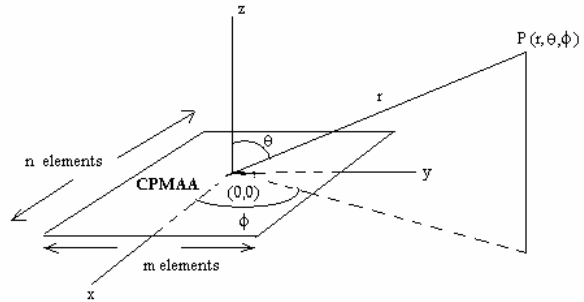


Fig. 1 Circular patch microstrip array antenna in z-plane

The array factor of the CPMAA is defined as [20]:

$$S_\theta(T_x, T_y) = \sum_{m=1}^{M-1} e^{j \frac{2\pi m b}{\lambda} (T_x + \frac{\Psi_x}{2\pi b / \lambda})} \times \sum_{n=1}^{N-1} e^{j \frac{2\pi n d}{\lambda} (T_y + \frac{\Psi_y}{2\pi d / \lambda})} = S_x S_y \quad (6)$$

Where  $b$  = spacing between elements in the  $x$  – direction

$d$  = spacing between element in the  $y$  – direction

$$T_x = \sin \theta \cos \phi$$

$$T_y = \sin \theta \sin \phi$$

The total far field of the array is given by:

$$E = E_e(T_x, T_y) S(T_x, T_y) \quad (7)$$

Basically the ability to receive the KU-band signals is all depends on the array factor. The separation of each element is very important as this would affect the gain and radiation pattern of the circular patch microstrip array antenna.

III. FEED NETWORK DESIGN

In this circular patch microstrip array antenna, each element is connected by a microstrip line which transforms the impedance of the patch into 50Ω. If we have 36 elements, a complex network is formed. This complex network is known as corporate-feed network [21], at which each element will be connected to the feed transmission lines. The corporate-feed network is used to provide power splits of 2<sup>n</sup> (i.e. n=2, 4, 8, 16, 32, etc.) [22]. This is accomplished by using either tapered lines to match the impedance of the elements to 50Ω coaxial or using quarter wavelength impedance transformer [23].

Corporate-feed networks are general and versatile. With this method, the model has more control on the feed of each element (amplitude and phase) and it is ideal for scanning phased arrays, multibeam arrays, or shaped-beam arrays.

Those who have been designing and testing microstrip arrays indicate that radiation from the feed line, using corporate-feed network, is a serious problem that limits the cross-polarisation and side lobe level of the arrays [24].

To understand more detail about the feed network design, one must understand the impedance and mutual coupling.

IV. IMPEDANCE OF THE CIRCULAR PATCH MICROSTRIP ARRAY ANTENN

Looking at the current (magnetic field) and voltage (electrical field) for a single circular patch, the current is maximum at the centre and minimum near the left and right edges, while the electrical field is zero at the centre and maximum near the left and minimum near the right edges [25], as in Fig. 2.

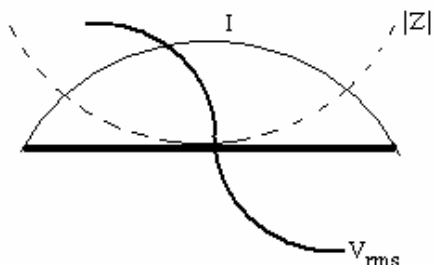


Fig. 2 Voltage, current and impedance distribution at resonant

From the magnitude of the current and voltage, we can conclude that the impedance is minimum at the middle of the patch and maximum (around 200Ω, but depend on the Q of the leaky cavity) near the edges. Hence, there is a point where the impedance is 50Ω along the “resonant length” at x-axis of the element.

Mathematically speaking, we can compute the impedance if we know the current distribution [26]:

$$I = \int_s \bar{J} \cdot d\bar{s} \tag{8}$$

$$Z = \frac{1}{2} \frac{P_{tot}}{|I|^2} \tag{9}$$

Where *J* = current density

*Z* = impedance

*P<sub>tot</sub>* = total power received

V. MUTUAL COUPLING

The geometry used in the calculation of the mutual coupling is shown in Fig. 3 by considering two neighbouring circular patches.

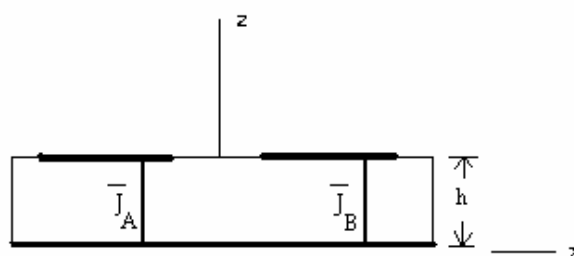


Fig. 3 Model used for mutual coupling analysis

In order to obtain an expression for the mutual coupling between adjacent elements, the reciprocity theorem in conjunction with the equivalence principle has been applied to simplify the problem to that of calculating the reaction between two magnetic current rings located at the centre of the substrate. A general discussion of the equivalent principle and the reciprocity theorem can be found in [27].

For a general two port network, the mutual impedance is written as:

$$Z_{12} = \frac{V_1}{i_2} \Big|_{i_2=0} \tag{10}$$

Where *i<sub>2</sub>* = current in the second circular patch  
*V<sub>1</sub>* = voltage appear at the first circular patch  
*Z<sub>12</sub>* = coupling impedance between the two circular patches

The voltage is given by:

$$V_1 = - \int_{-h}^0 \bar{E}[\bar{J}] \cdot \bar{z} dz \tag{11}$$

The more accurate expression for the impedance of the circular microstrip patch antenna can be found in [28].

VI. RESULTS

Fig. 4 shows the design of circular patch array antenna and Fig. 5 shows the 3D view of the antenna. Fig.6 is the input reflection coefficient of the circular patch array antenna and Fig. 7 is the radiation pattern of the antenna. The gain is shown in Fig. 8.

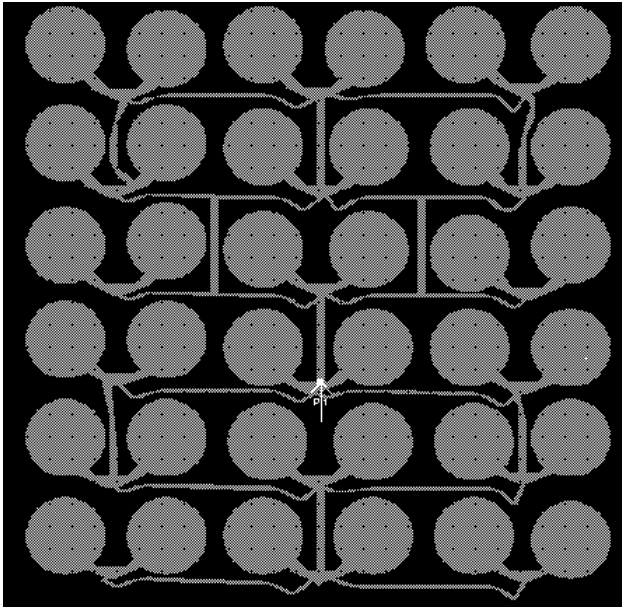


Fig. 4 36 elements circular patch microstrip array antenna

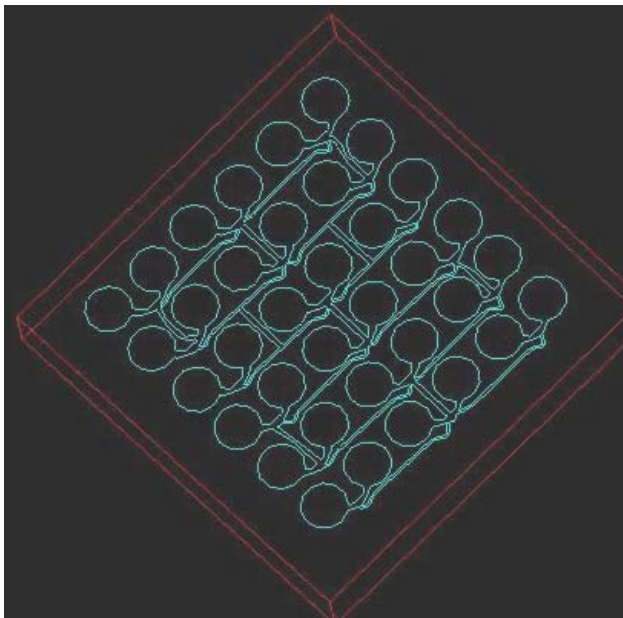


Fig. 5 A 3D of 36 elements circular patch microstrip array antenna

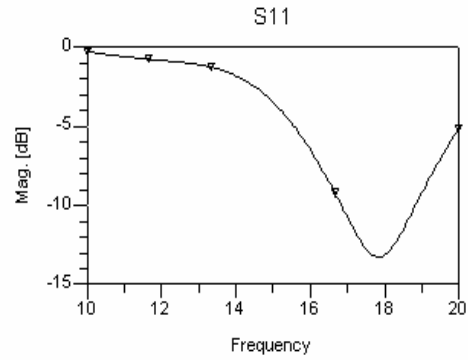


Fig. 6 The input reflection coefficient of the circular patch microstrip array antenna

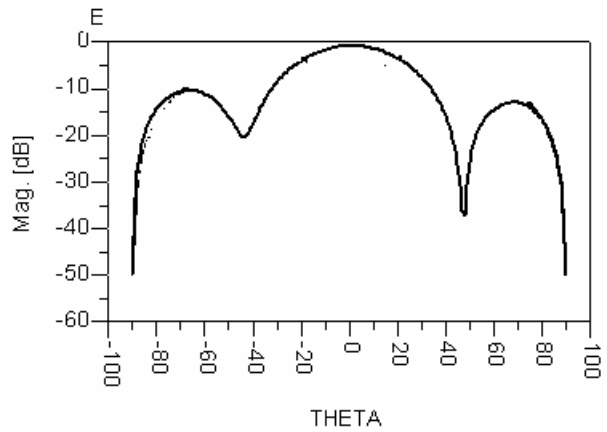


Fig. 7 The radiation pattern

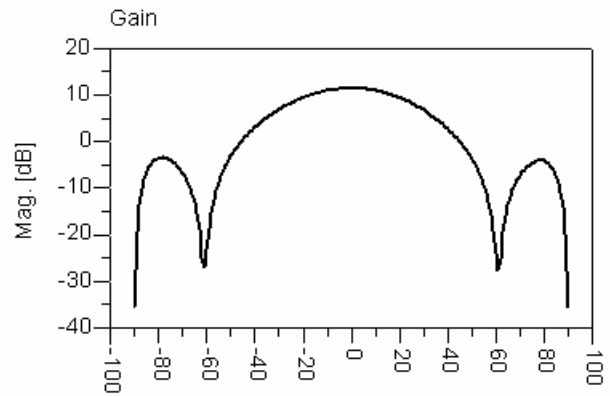


Fig. 8 The Gain

As seen from the simulation results, especially the  $S_{11}$  parameter. It can tell us that this antenna will get resonance at 18 GHz even though the design frequency is 15 GHz. The gain of the antenna is 10 dB in  $0^\circ$  direction. This is optimum gain under  $\epsilon_r = 2.33$  using alumina and the thickness of the substance is 1.6mm.

Note that the actual size of the antenna is  $7.2 \text{ cm} \times 7.2 \text{ cm}$ . When using ADS to optimize the gain. It shows that the size of the antenna is  $30 \text{ cm} \times 30 \text{ cm}$  with each element's radius is  $2.29 \text{ cm}$ . The spacing between each element is  $0.5 \text{ cm}$ .

## VII. CONCLUSION

From the simulation results, we can see that the gain perhaps can be improved by increased the number of elements.

It is also seen that the CPMAA is very narrow bandwidth.

All the results simulated are the optimum values which are generated by ADS. Changing the parameter like substance's thickness, material, tangent loss and dielectric constant does effect the gain performance of the antenna.

## ACKNOWLEDGMENT

Our sincerest appreciation must be extended to the INTI International University College which gives a full financial support to present this paper. We wish to thank the University of Malaya, Faculty of Engineering, which give a support and approval of this project.

## REFERENCES

- [1] G. O. Young, "Synthetic structure of industrial plastics (Book style with paper title and editor)," in *Plastics*, 2nd ed. vol. 3, J. Peters, Ed. New York: McGraw-Hill, 1964, pp. 15–64.
- [2] W.-K. Chen, *Linear Networks and Systems* (Book style). Belmont, CA: Wadsworth, 1993, pp. 123–135.
- [3] H. Poor, *An Introduction to Signal Detection and Estimation*. New York: Springer-Verlag, 1985, ch. 4.
- [4] B. Smith, "An approach to graphs of linear forms (Unpublished work style)," unpublished.
- [5] E. H. Miller, "A note on reflector arrays (Periodical style—Accepted for publication)," *IEEE Trans. Antennas Propagat.*, to be published.
- [6] J. Wang, "Fundamentals of erbium-doped fiber amplifiers arrays (Periodical style—Submitted for publication)," *IEEE J. Quantum Electron.*, submitted for publication.
- [7] C. J. Kaufman, Rocky Mountain Research Lab., Boulder, CO, private communication, May 1995.
- [8] Y. Yorozu, M. Hirano, K. Oka, and Y. Tagawa, "Electron spectroscopy studies on magneto-optical media and plastic substrate interfaces (Translation Journals style)," *IEEE Transl. J. Magn. Jpn.*, vol. 2, Aug. 1987, pp. 740–741 [*Dig. 9<sup>th</sup> Annu. Conf. Magnetism Japan*, 1982, p. 301].
- [9] M. Young, *The Technical Writers Handbook*. Mill Valley, CA: University Science, 1989.
- [10] J. U. Duncombe, "Infrared navigation—Part I: An assessment of feasibility (Periodical style)," *IEEE Trans. Electron Devices*, vol. ED-11, pp. 34–39, Jan. 1959.
- [11] S. Chen, B. Mulgrew, and P. M. Grant, "A clustering technique for digital communications channel equalization using radial basis function networks," *IEEE Trans. Neural Networks*, vol. 4, pp. 570–578, July 1993.
- [12] R. W. Lucky, "Automatic equalization for digital communication," *Bell Syst. Tech. J.*, vol. 44, no. 4, pp. 547–588, Apr. 1965.
- [13] S. P. Bingulac, "On the compatibility of adaptive controllers (Published Conference Proceedings style)," in *Proc. 4th Annu. Allerton Conf. Circuits and Systems Theory*, New York, 1994, pp. 8–16.
- [14] G. R. Faulhaber, "Design of service systems with priority reservation," in *Conf. Rec. 1995 IEEE Int. Conf. Communications*, pp. 3–8.
- [15] W. D. Doyle, "Magnetization reversal in films with biaxial anisotropy," in *1987 Proc. INTERMAG Conf.*, pp. 2.2-1–2.2-6.
- [16] G. W. Juette and L. E. Zeffanella, "Radio noise currents in short sections on bundle conductors (Presented Conference Paper style)," presented at the IEEE Summer power Meeting, Dallas, TX, June 22–27, 1990, Paper 90 SM 690-0 PWRs.
- [17] J. G. Kreifeldt, "An analysis of surface-detected EMG as an amplitude-modulated noise," presented at the 1989 Int. Conf. Medicine and Biological Engineering, Chicago, IL.
- [18] J. Williams, "Narrow-band analyzer (Thesis or Dissertation style)," Ph.D. dissertation, Dept. Elect. Eng., Harvard Univ., Cambridge, MA, 1993.
- [19] N. Kawasaki, "Parametric study of thermal and chemical nonequilibrium nozzle flow," M.S. thesis, Dept. Electron. Eng., Osaka Univ., Osaka, Japan, 1993.
- [20] J. P. Wilkinson, "Nonlinear resonant circuit devices (Patent style)," U.S. Patent 3 624 12, July 16, 1990.
- [21] *IEEE Criteria for Class IE Electric Systems* (Standards style), IEEE Standard 308, 1969.
- [22] *Letter Symbols for Quantities*, ANSI Standard Y10.5-1968.
- [23] R. E. Haskell and C. T. Case, "Transient signal propagation in lossless isotropic plasmas (Report style)," USAF Cambridge Res. Lab., Cambridge, MA Rep. ARCRL-66-234 (II), 1994, vol. 2.
- [24] E. E. Reber, R. L. Michell, and C. J. Carter, "Oxygen absorption in the Earth's atmosphere," Aerospace Corp., Los Angeles, CA, Tech. Rep. TR-0200 (420-46)-3, Nov. 1988.
- [25] (Handbook style) *Transmission Systems for Communications*, 3rd ed., Western Electric Co., Winston-Salem, NC, 1985, pp. 44–60.
- [26] *Motorola Semiconductor Data Manual*, Motorola Semiconductor Products Inc., Phoenix, AZ, 1989.
- [27] (Basic Book/Monograph Online Sources) J. K. Author. (year, month, day). *Title* (edition) [Type of medium]. Volume(issue). Available: [http://www.\(URL\)](http://www.(URL))
- [28] J. Jones. (1991, May 10). *Networks* (2nd ed.) [Online]. Available: <http://www.atm.com>